Effect of dissolved oxygen concentration on microalgal culture in photobioreactors

A. Kazbar, Guillaume Cogne, B. Urbain, H. Marec, B. Le-Gouic, J. Tallec, H. Takache, A. Ismail, Jeremy Pruvost

Effect of dissolved oxygen concentration on microalgal culture in photobioreactors

Article *in* Algal Research · February 2019

DOI: 10.1016/j.algal.2019.101432

CITATIONS
4

READS
974

9 authors, including:

Antoinette Kazbar
Wageningen University & Research
4 PUBLICATIONS **5** CITATIONS
SEE PROFILE

Guillaume Cogne
University of Nantes
22 PUBLICATIONS **749** CITATIONS
SEE PROFILE

Hosni Takache
Lebanese University
18 PUBLICATIONS **312** CITATIONS
SEE PROFILE

A. Ismail
Lebanese University
22 PUBLICATIONS **418** CITATIONS
SEE PROFILE

Effect of dissolved oxygen concentration on microalgal culture in photobioreactors

A. Kazbar[a,b,c], G. Cogne[a], B. Urbain[a], H. Marec[a], B. Le-Gouic[a], J. Tallec[a], H. Takache[b], A. Ismail[b], J. Pruvost[a,*]

[a] GEPEA, Université de Nantes, CNRS, UMR6144, bd de l'Université, CRTT, BP 406, 44602 Saint-Nazaire Cedex, France
[b] Department of Food Science and Technology, Faculty of Agricultural and Veterinary Medicine, Lebanese University, Dekweneh, Beirut, Lebanon
[c] Platform for Research and Analysis in Environmental Sciences, Doctoral School of Science and Technology, Faculty of Sciences, Lebanese University, P.O Box 5, Campus Rafic Hariri, Hadath, Beirut, Lebanon

ARTICLE INFO

Keywords:
Dissolved oxygen
Productivity
Microalgae
Photobioreactor
Modeling

ABSTRACT

High concentrations of dissolved oxygen can inhibit the growth of photosynthetic microorganisms in microalgal culture systems. Not taking into account this parameter can also affect the reliability of mathematical models predicting biomass productivity. This study investigates the impact of high dissolved oxygen concentrations (C_{O_2}) on biomass productivity. The eukaryotic microalgae *Chlorella vulgaris* was cultivated in a torus-shaped photobioreactor in chemostat mode at constant light and for different C_{O_2}. Results showed a loss of biomass productivity at $C_{O_2} \geq 31\ g{\cdot}m^{-3}$. By recalculating the specific rate of cofactor regeneration on the respiratory chain (J_{NADH_2}), the kinetic growth model was able to predict the impact of C_{O_2}. This improved model was then used to explain the discrepancy in performances between two photobioreactor geometries, highlighting the utility of regulating gas-liquid mass transfer via aeration for better optimization of photobioreactor performances.

1. Introduction

During phototrophic growth, microalgae consume carbon dioxide (CO_2) and produce oxygen (O_2). The evolved oxygen can easily build up to high concentrations in geometries like closed photobioreactors (PBRs), and this can have a negative effect on biomass productivity by inhibiting growth of the microalga cells. The main processes that can occur at high dissolved oxygen concentration (C_{O_2}) are generally attributed to photorespiration, Mehler reaction (water-water cycle) and photoinhibition [1]. Photorespiration is defined as the light-dependent consumption of oxygen and production of CO_2 [2]. It results from the oxygenase reaction catalyzed by ribulose-1,5-bisphosphate carboxylase/oxygenase (RuBisCO) [3,4]. Photoinhibition occurs when microalgae are exposed to high light intensities for a long period, and leads to the generation of reactive oxygen species (ROS) that can damage cellular components [5]. In these conditions, high C_{O_2} can play a positive role by dissipating excess energy through Mehler reactions [6,7].

Raso et al. [8] demonstrated that in sub-saturating light intensities, *Nannocchloropsis sp* showed a loss of productivity in 250% air-saturated dissolved oxygen solution. Their study showed also a decrease in the photosynthetic efficiency with increasing C_{O_2}, which was a result of a photorespiration activity. The same conclusions were drawn by Sousa et al. [9], where a loss in biomass productivity was only explained by the photorespiration activity of RuBisCO since light was in sub-saturating values. Pigment concentration was not affected by C_{O_2}, thus indicating no significant photooxidative damage. Costache et al. [10] investigated the effect of C_{O_2} on growth of *Neochloris oleoanbudans* at high light intensities and found that the loss of microalgae biomass productivity was the result of both photooxidative (photoinhibition) and photorespiration activities.

Excessive concentrations of dissolved oxygen could be avoided by effective air stripping to evacuate oxygen from the cultivation system. However, special attention needs to be paid to maintain a sufficiently high concentration of dissolved carbon in the culture medium, typically by simultaneously injecting CO_2. In fact, according to Genkov & Spreitzer [11], RuBisCO has 17-fold higher affinity for CO_2 than O_2 for the microalga *Chlamydomonas reinhardtii*. Maintaining a high concentration of dissolved carbon in microalgal culture systems can thus reduce the impact of O_2-dependent photorespiration activity on microalgal photosynthetic growth.

C_{O_2} is also a function of the culture system design, specifically its

gas-liquid mass transfer efficiency [12,13]. Tubular photobioreactors and raceways can accumulate high concentrations of dissolved oxygen [14,15,45] as gas-liquid mass transfer efficiency is low in these two geometries. This makes it relevant to carefully design and optimize culture systems to maintain optimum CO_2 and O_2 dissolved concentrations.

Microalgal culture system engineering has made huge strides in recent years. Mathematical modeling is useful in that regard to optimize and scale microalgal culture systems. Co-authors developed for that purpose a knowledge model for predicting the biomass productivity of light-limited microalgae cultures in PBRs [16–18]. The knowledge model combines radiative transfer and photosynthetic growth models. By describing the light attenuation within the culture bulk as a function of parameters affecting light transfer, such as biomass concentration and microalgal radiative properties, a coupling can be made with a kinetic model of photosynthetic growth, making it possible to calculate the resulting mean volumetric biomass production rate $\langle r_x \rangle$ and ultimately the biomass concentration (C_X) and PBR biomass productivity (P_X) as a function of operating conditions such as photon flux density (PFD) or dilution rate D (h^{-1}) in continuous chemostat culture mode.

This study aims to quantify the negative effect of C_{O_2} on PBR kinetic performances (i.e. biomass productivity) and investigate the related impact on growth model parameters. The study was conducted for the eukaryotic microalgae *Chlorella vulgaris* grown at chemostat mode for a photon flux density (PFD) of 250 µmol/m^2/s and a dilution rate D of 0.02 h^{-1}. To investigate the effect of PBR design, experiments were conducted in an airlift PBR and in a torus-shaped PBR system. The latter combines both mechanical stripping and aeration. This allowed control of the gas-liquid mass transfer rate independently of the need to guarantee adequate mixing in the culture volume [19]. This study was concluded by analyzing the role of the gas-liquid mass transfer in various PBR geometries in order to highlight their capacity to accumulate dissolved oxygen.

2. Material and methods

2.1. Experimental setup

2.1.1. Selected strain

The strain used in this study is the eukaryotic microalgae *Chlorella vulgaris* (211/19, SAG collection, Germany). The autotrophic Sueoka medium was used with N-NH_4^+ as nitrogen source. It contains in (g/l): NH_4Cl 1.45, $MgSO_4$, $7H_2O$ 0.281, $CaCl_2$, $2H_2O$ 0.05, KH_2PO_4 0.609, $NaHCO_3$ 1.68 and 1 mL of Hunter's trace elements solution [20]. Nutrient concentrations were adjusted to avoid mineral limitation and guarantee that growth was only light-limited [17].

2.1.2. Cultivation system

Two PBR geometries were used, i.e. a torus-shaped PBR and a flat-panel airlift system. The torus-shaped PBR has been designed for lab-scale experiments requiring tight control of culture conditions [21]. One of its main features is to allow a broad range of variation in gas-liquid mass transfer efficiency; in fact, the culture is mechanically circulated via rotation of a marine impeller together with low air bubbling at controlled flow-rate. As mixing is mainly provided by mechanical stirring, low flow-rate can be applied. This was found to be valuable for studies requiring accurate gas analysis [19]. If necessary, more intense gas bubbling could obviously be applied, so as to increase the gas-liquid mass transfer rate. Because of the accurate control of culture conditions, the torus PBR has been widely used in recent years for in-depth studies and kinetic model setting, including for the optimization of microalgal biomass productivity [17,18] and the investigation of light/dark cycles effect on microalgal growth [22]. Here we extend its use to investigate the effect of C_{O_2} on microalgal growth.

The torus PBR was built from PMMA (polymethyl methacrylate) and is thus fully transparent. The front surface is plane and the torus channel is square-sectioned with a depth of culture L_Z = 0.04 m, leading to a reactor volume $V_{PBR} = 1.5.10^{-3}$ m^3 and a specific illuminated area $a_{light} = S/V_{PBR}$ of 25 m^{-1} [21]. The torus PBR can receive a complete loop of common sensors and automations. Temperature and pH were monitored and regulated continuously (Mettler Toledo, Inpro 4801SG, France sensor). The former was regulated by a circulation of a thermoregulated water in a double jacket at the rear of the PBR. The latter was regulated by a CO_2 gas injection from a gas bottle (Airliquide, 98% CO_2). CO_2 temperature and moisture was not controlled. C_{O_2} was measured using an oxygen probe (Pyroscience, P-FSO2-MINI-ST, Germany). Gas injection of CO_2 and N_2 was controlled and regulated by a mass flowmeter (Bronkhorst HIGH-TECH, Bronkhorst, Netherlands).

The flat-panel airlift PBR has a $V_{PBR} = 10^{-3}$ m^3 and L_z = 0.03 m, giving an $a_{light} = S/V_{PBR}$ of 33.3 m^{-1}. Mixing was only obtained by air injection [23]. For this geometry, temperature was regulated at 25 °C by a heating plate in the back of the PBR and pH was regulated at 7.5 by automatic injection of CO_2 from a gas bottle (Airliquide, 98% CO_2).

The torus and airlift PBRs were exposed to PFD = 250 µmol/m^2/s via LED panels designed to produce homogeneous white light [17]. C_{O_2} was modulated by bubbling gaseous nitrogen (N_2) at a given flowrate regulated by a Bronkhorst HIGH-TECH flowmeter (Bronkhorst, France). Experiments were conducted in continuous chemostat mode for the same dilution rate (D = 0.02 h^{-1}). This dilution rate corresponds to a residence time of 50 h. Therefore, steady-state was reached 11 days after inoculation (i.e. five time the residence time). For each C_{O_2}, biomass concentration (C_X), pigment concentration and inorganic carbon concentration were measured. Volumetric gas-liquid mass transfer, k_La, was also measured for each flowrate (see next section).

2.1.3. Biomass dry weight concentration

Depending on cell concentration, 0.4–10 mL of algal suspension was filtered through a pre-dried pre-weighed glass-fiber filter (Whatman GF/F, 0.7 µm). Biomass concentrate was washed with distilled water to eliminate minerals. The filter was dried at 110 °C for 24 h, cooled in a desiccator, and reweighed. Final value was the average of three replicates and the error bars correspond to the standard deviation. Biomass concentrations were used to deduce biomass productivities from residence dilution rate D (i.e. volumetric biomass productivity $P_X = C_X.D$).

2.1.4. Pigment contents

Culture samples of volume V_1 were centrifuged at 13,400 rpm for 10 min. The pellet was suspended in a volume V_2 of methanol then stored in the dark at 44 °C for 45 to 180 min to allow complete extraction. Cell fragments were then separated by centrifuging at 13,400 rpm for 10 min, and the optical density of the supernatant containing the pigments dissolved in methanol was measured with a spectrophotometer at 480, 652, 665 and 750 nm (Jenway, England or Safas MC2, Monaco). Three replicates were prepared, and chlorophyll *a*, b and photoprotective carotenoids (PPC) concentrations were determined using the following relationships [24]:

$$C_{Chla} = [-8.0962(DO_{652} - DO_{750}) + 16.5169\,(DO_{665} - DO_{750})] \times {V_{methanol}}/{V_{culture}} \quad (1)$$

$$C_{Chlb} = [27.4405(DO_{665} - DO_{750}) + 12.1688\,(DO_{665} - DO_{750})] \times {V_{methanol}}/{V_{culture}} \quad (2)$$

$$C_{PPC} = [4(DO_{480} - DO_{750})] \times {V_{methanol}}/{V_{culture}} \quad (3)$$

2.1.5. Inorganic carbon concentration determination

Inorganic carbon concentration in PBRs was determined offline using a COTmeter (SHIMADZU TOC5000A, Japan). 10 mL of a culture sample was taken and filtered with a 0.2-µm Minisart® Syringe Filter.

Thee samples were introduced via an injector into a combustion tube. Then inorganic carbon concentration was measured by the analyzer.

2.1.6. Dissolved oxygen concentration measurement

C_{O_2} in PBRs was obtained online from an optical oxygen sensor (Pyroscience FireSting O_2-Mini) using REDFLASH technology, which is based on red light excitation of REDFLASH indicators showing luminescence in the near-infrared (NIR) which decreases with increasing oxygen concentration (quenching effect). The sensor system is connected to a FireSting O_2 fiber-optic oxygen meter and is PC-controlled.

2.2. Theoretical considerations

2.2.1. Overview of the light-limited kinetic growth model

Algal biomass growth rate is the net result of photosynthesis and endogenous respiration. Predicting the rate of both mechanisms is a challenging task due to the manifold parameters affecting biomass growth rate, such as temperature, pH, light intensity, nutrient availability and C_{O_2} [25].

Here we used a kinetic growth model able to very accurately represent the effect of light attenuation conditions on resulting productivity [16]. This model was however restricted to light effect (i.e. no effect of dissolved oxygen) and for a growth on nitrate (NH_4^+) as nitrogen source. A full description of this model can be found in the Appendix. The model expresses the local rate of oxygen production J_{O_2} as a function of the rate of photon absorption (A):

$$J_{O_2} = J_{O_2,photo} - J_{O_2,resp} = \left[\rho_M \overline{\phi'}_{O_2} \frac{K \cdot A}{K + A} - \frac{J_{NADH_2}}{\nu_{NADH_2-O_2}} \frac{K_r}{K_r + A} \right] \quad (4)$$

where $J_{O_2,photo} = \rho_M \overline{\phi'}_{O_2} \frac{K \cdot A}{K + A}$ represents the photosynthetic term. $\rho_M$is the maximum energy yield for photon conversion, $\overline{\phi'}_{O_2}$ is the mean mass quantum yield for the *Z*-scheme of photosynthesis, K is the half saturation constant for photosynthesis and A—the local specific rate of photon absorption. Respiration term was represented as $J_{O_2,resp} = \frac{J_{NADH_2}}{\nu_{NADH_2-O_2}} \frac{K_r}{K_r + A}$ where J_{NADH_2} is the specific rate of cofactor regeneration on the respiratory chain, linked to oxygen consumption by the stoichiometric coefficient $\nu_{NADH_2-O_2}$ (stoichiometric coefficient of cofactor regeneration on the respiratory chain), and K_r is a saturation constant describing the inhibition of respiration in light.

Once $\langle J_{O_2} \rangle$ is known, the mean volumetric biomass growth rate $\langle r_x \rangle$ can be retrieved directly using the stoichiometry relating oxygen and biomass productions:

$$\langle r_x \rangle = \frac{\langle J_{O_2} \rangle C_X M_X}{\nu_{O_2-X}} \quad (5)$$

It can be then be combined with a mass balance onto the PBR to predict its productivity.

$$\frac{dC_x}{d_t} = \langle r_x \rangle - D \cdot C_X \quad (6)$$

where $\langle r_x \rangle$ is biomass growth rate, D is dilution rate and C_X is biomass concentration given in kg/m^3.

Once steady state is reached, $\frac{dC_x}{d_t} = 0$, thus:

$$\langle r_x \rangle = D \cdot C_X = P_X \quad (7)$$

This equation was also used to experimentally determine biomass productivity P_X from biomass concentration measurement (C_X). Note that the same approach as Eq. (5) can be used to obtain averaged photosynthetic ($\langle J_{O_2,photo} \rangle$) or respiration ($\langle J_{O_2,resp} \rangle$) contributions, and then calculate J_{NADH_2} from Eq. (4) (see Section 2.2.3).

2.2.2. Kinetic growth model for Chlorella vulgaris

Following Takache et al. [18] who modeled *Chlamydomonas reinhardtii* growth, the kinetic growth model for *Chlorella vulgaris* was established by Souliès et al. [17]. Co-authors experiments were performed in a similar torus PBR to that the one used here, and in continuous mode, for a constant PFD = 200 µmol/m^2/s and for different dilution rates. For each experiment, the dry biomass C_x and volumetric productivity P_x were determined at steady state (Eq. (7)). This allowed to determine the kinetic growth model parameters of *Chlorella vulgaris*, as summarized in Souliès et al. [17] and given in Appendix here.

2.2.3. Experimental determination of J_{NADH_2}

J_{NADH_2} is the specific rate of the cofactor regeneration, and is directly related to respiratory activity. It was retrieved in our study from both the kinetic growth model and experimental measurements. Dry-weight biomass concentration in steady state was used to determine biomass productivity (Eq. (7)). The experimental productivity rate served to then calculate the experimental rate of oxygen production J_{O_2} using Eq. (5).

By assuming that parameters of the photosynthetic term $J_{O_2,photo}(\rho_M, \overline{\phi'}_{O_2}, K)$ were the same as determined by Souliès et al. [17], the oxygen consumption rate due to respiration, $J_{O_2,resp}$ can thus be calculated using Eq. (4). In this equation, parameter K_r is not independent and can be linked to the specific rate of cofactor regeneration on the respiratory chain by the definition of the compensation point of photosynthesis. This compensation point is obtained for a photon absorption rate value A_c leading to null net oxygen production (i.e. $J_{O_2} = 0$). In our case, we considered the same compensation point as determined by previous authors (A_c = 2800 $\mu mol_{hv}/kg/s$). Thus, $J_{NADH_2}$was determined as follows:

$$J_{NADH_2} = \langle J_{O_2,resp} \rangle \cdot \nu_{NADH_2-O_2} \left[\frac{1}{\left\langle \frac{K_r}{K_r + A_c} \right\rangle} \right] \quad (8)$$

In this way, J_{NADH_2} can be retrieved for each experimental datapoint, and thus each of the C_{O_2} conditions.

2.2.4. Estimation of photorespiration activity

Photorespiration occurs when high concentrations of oxygen and/or low concentrations of CO_2 are present [1,4]. In this condition, RuBisCO reacts with oxygen instead of CO_2. When RuBisCO fixes CO_2, two molecules of glycerate 3-phosphate are formed [26], then converted in the central carbon metabolism to form biomass components. However, if only oxygen is fixed, one glycerate 3-phosphate is formed and one molecule of glycolate 2-phosphate is formed. The synthesis of glycolate 2-phospate dissipates energy in the form of ATP. This costs additional ATP and NADPH which are generated in the light reaction of photosynthesis. As a result, less energy is available for growth, decreasing the yield of microalgal biomass production.

Photorespiration activity can be related to CO_2-to-O_2 concentration ratio, here denoted $\tilde{r}$, assuming in first approximation as representative of the RuBisCO environment. It is the ratio between the molar concentration of dissolved CO_2 to molar concentration of dissolved O_2 (Eq. (9)). CO_2 concentration is given as a function of pH and total dissolved inorganic carbon concentration (DIC), so that CO_2/O_2 concentration ratio can be defined as follows:

$$r = \frac{C_{CO_2}}{C_{O_2}} = \frac{DIC/_{K'}}{C_{O_2}} \quad (9)$$

where K' is the dissociation constant of CO_2 in water, equal to 14.5 at pH = 7.5, C_{CO_2} is the molar concentration of dissolved carbon dioxide in mol_{CO2}/L, and C_{O_2} is the molar concentration of dissolved oxygen in mol_{O2}/L.

Based on the knowledge of relative specificity of RuBisCO as discussed in Raso et al. [8], Urbain [27] has estimated photorespiration activity for different CO_2/O_2 concentration ratios and its influence on relative biomass productivity (see Fig. 1), showing that photorespiration activity can typically occur at CO_2/O_2 ratios lower than 0.4, but at

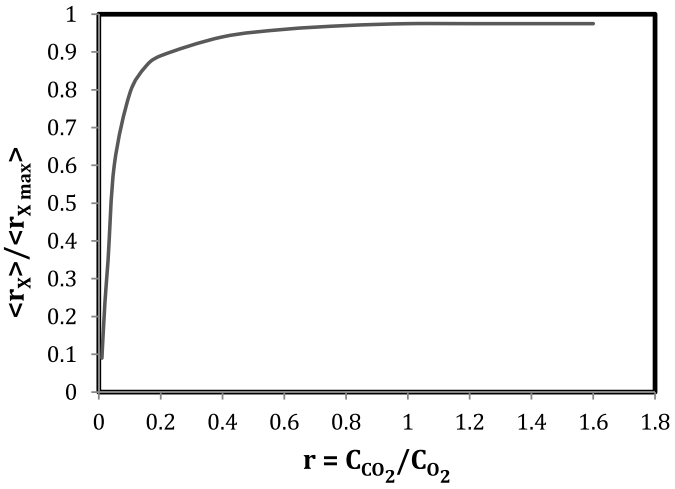

Fig. 1. Impact of photorespiration on the relative biomass productivity [27].

a ratio > 0.6, it has negligible effect on biomass productivity ($< 10\%$). This clearly underlines how the effects of photorespiratory pathway might often be neglected under standard PBR operating conditions (i.e. sufficient CO_2 supply).

Assuming that RuBisCO has 17-fold higher affinity for CO_2 than O_2, as shown for *Chlamydomonas reinhardtii* by Genkov & Spreitzer [11], and that the carbon concentrating mechanisms (CCM) could keep the CO_2 concentration near RuBisCO high enough to reduce the oxygenase flux, photorespiration should not present any significant inhibitory effect on microalgal growth. To guarantee this condition, 20 mM of $NaHCO_3$ was added to the medium. As shown later, this was found sufficient to obtain an "r" ratio in a range where photorespiration presents negligible effect ($r > 0.6$).

2.2.5. Gas-liquid mass transfer determination

Gas-liquid mass transfer in the cultivation system has a direct influence on the C_{O_2} obtained in the bulk of the culture [28]. It is characterized by the volumetric mass transfer coefficient k_La (h^{-1}), which was experimentally obtained at 25 °C using a de-oxygenation/re-oxygenation method [29] that consists in removing dissolved oxygen from the liquid phase by injecting gaseous nitrogen (N_2), then monitoring the increase in C_{O_2} when switching back to air injection. During the re-oxygenation phase, mass balance on dissolved oxygen yields the following equation [30]:

$$N_{O_2} = \frac{d_{C_L}}{dt} = K_L{\cdot}a\ (\ C^*_{O_2} - C_{O_2}) \tag{10}$$

where N_{O2} (g O_2/m^3/h) is oxygen mass transfer rate, C_{O_2} is dissolved oxygen concentration, and $C_{O_2}{}^*$ is dissolved oxygen concentration at equilibrium with the gas phase (8.25 g/m^3 with air at 25 °C).

By integrating this equation, assuming time-constant conditions of mass transfer (i.e. constant k_La over the experiment), the following equation is obtained, which allows the volumetric mass transfer coefficient k_La to be calculated from the time-course of C_{O_2} measurements:

$$ln\frac{(C^*_{O_2} - C_{O_2})}{(C^*_{O_2} - C_{O_2,\,i})} = -K_L{\cdot}a{\cdot}t \tag{11}$$

where $C_{O_2,\,i}$ is initial C_{O_2}, as obtained before air injection ($C_{O_2,\,i} = 0$ in nitrogen bubbling condition). Measurement of volumetric mass transfer coefficient was made under the same medium conditions used in experiments.

2.2.6. Theoretical determination of dissolved oxygen concentration

In order to investigate the gas-liquid mass transfer performance of different photobioreactor geometries, an approach was used based on comparing oxygen production during photosynthetic growth against the oxygen physically transferable from liquid to gas phases [31]. This approach was also applied by Pruvost et al. [30] to investigate the mass transfer performance of an intensified PBR, the Algofilm© PBR. Oxygen production rate(P_{O_2}) being proportional to growth rate and volumetric productivity (P_V), we then obtain at steady state:

$$P_{O_2} = Y_{O_2/_X}{\cdot}P_V \tag{12}$$

where $Y_{O_2/_X}$ is specific yield of oxygen production (1.5 kg of oxygen per kg of biomass for *Chlorella vulgaris*; [30]).

Biological oxygen rate has to be compared with the aeration performance of the PBR, as represented by the volumetric mass transfer coefficient k_La and given by Eq. (10). Under stead- state conditions, a mass balance for oxygen leads to:

$$N_{O_2} = P_{O_2} \tag{13}$$

This enables us to calculate the dissolved oxygen concentration in the culture medium at steady-state conditions:

$$C_{O_2} = \frac{Y_{O_2/_X}.\ P_X}{K_L a} + C^*_{O_2} \tag{14}$$

3. Results and discussion

3.1. Experimental investigation of the effect of C_{O_2} on Chlorella vulgaris growth

3.1.1. Biomass productivity as a function of C_{O_2}

The torus PBR was used to characterize the impact of different C_{O_2} on biomass productivity. It consisted of continuous culture in chemostat mode for a constant dilution rate D = 0.02 h^{-1} and PFD = 250 µmol/m^2/s. Concentrations of dissolved oxygen were varied by modulating N_2 gaseous flowrate injected in the culture bulk.

Fig. 2 shows surface productivity of *Chlorella vulgaris* obtained as a function of C_{O_2}. *At* a C_{O_2} between 8 g/m^3 and 25 g/m^3, influence on surface productivity was negligible, but for C_{O_2} at 31 g/m^3 there was a 30% loss in productivity. At higher C_{O_2} values, the PBR became unstable, and the culture was lost (data not shown in Fig. 2).

Our results confirm several studies highlighting the effect of a high C_{O_2} on microalgal growth [8–10]. These studies have shown that a $C_{O_2} > 25$ g/m^3 can inhibit eukaryotic microalgae growth. This inhibition could result from many metabolic processes. Kliphuis et al. [1] demonstrated that when photoinhibition was avoided (i.e. at sub-saturating light intensities), photorespiration was the main process

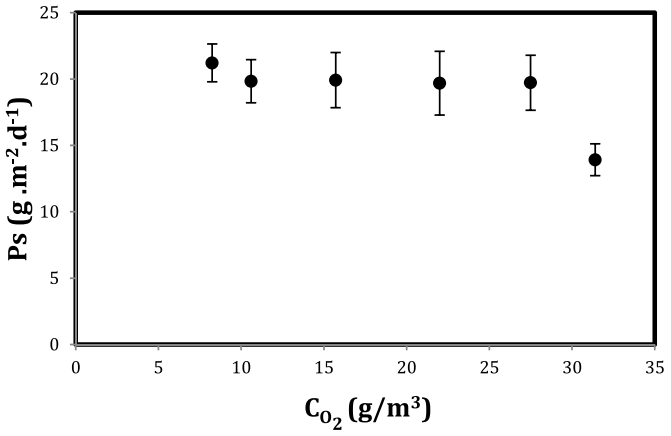

Fig. 2. Evolution of the surface productivity (P_s) of *Chlorella vulgaris* for different dissolved oxygen concentrations (C_{O_2}) in the torus PBR, for a photon flux density PFD = 250 $\mu mol_{hv}/m^2/s$ and a dilution rate D = 0.02 h^{-1} (data are shown as a mean ± SD, $n = 3$).

leading to a photosynthetic deficiency. However, in high light intensities, large dissolved oxygen concentrations led to photochemical damage of the photosynthetic apparatus and resulted in a decrease in pigment concentrations in microalgal cells [32]. We can note that we applied only sub-saturating PFD where we found a near- constant pigment content (5–7%), confirming that no significant photoinhibitory effect was obtained (see also Section 3.1.3).

3.1.2. Estimation of the ratio of photorespiration activity

Photorespiration ratios obtained for each experiment were calculated by Eq. (9). C_{O_2} was obtained using a dissolved oxygen concentration sensor and C_{CO_2} was obtained using COTmeter (SHIMADZU TOC5000A, Japan) measurements of inorganic carbon. Results showed that for a $C_{O_2} \approx 30\ g/m^3$, the ratio "r" was of 0.67. For this value, the 30% loss of biomass productivity occurred. Following Fig. 1, a negligible effect of photorespiration can then be expected (< 5%) sine the minimal ratio value for a significant photorespiration impact is of 0.2. In our case the photorespiration process was overcome by adding extra dissolved carbon (i.e. $NaHCO_3$).

Furthermore, as described in the previous section, we applied sub-saturating PFD ($250\ \mu mol \cdot m^{-2} \cdot s^{-1}$) which led to negligible photoinhibition. This tends to indicate that algal growth was mainly inhibited by oxygen via high respiration activity [9]. In fact, the cells show a different metabolic behavior at high C_{O_2} than at optimum growth conditions, with a decrease in the photosynthetic growth activity. Martzoff [33] investigated metabolic flows and showed that futile mechanisms could occur at high dissolved oxygen concentration. These mechanisms are accompanied by an increase in respiratory flow, resulting in a need for an increase in incoming photon flux to maintain the same biomass productivity (i.e. growth rate). Thus, part of the energy is dissipated by other mechanisms instead of producing biomass, resulting in a decrease of biomass growth rate for the same light conditions.

3.1.3. Pigment concentration as a function of C_{O_2}

Fig. 3 presents the total pigments and carotenoids contents of *Chlorella vulgaris* measured for the different C_{O_2} values. There was no significant effect of high C_{O_2}, and for all other C_{O_2} values. Carotenoid contents were around 1% DW (dry weight) and total pigment percentage was between 5.5% DW and 7.5% DW. This result confirms that light stress remains negligible, as otherwise it would have resulted in significant loss or damage in pigment apparatus due to photoacclimation processes [17]. In addition, there was no significant photooxidative damage to the photosynthetic apparatus. In fact, photoprotective carotenoids (PPC) are usually formed when an extra formation of oxygen radicals and singlet oxygen occurs. The accumulation of oxygen in the photobioreactor could induce the extra formation of oxygen radicals which would consequently damage the photosynthetic apparatus and induce extra carotenoids production to protect the cells. This phenomenon should be confirmed by fluorescent measurement [5]. In our experiments, the measurements of photosynthetic activity of *Chlorella vulgaris* represented by Fv/Fm gave values around 0.7 for all C_{O_2} levels. For green algae, Fv/Fm ratio is between 0.7and 0.8 in normal growth conditions [34]. The same conclusions were obtained for *Neochloris oleoabundans* in which chlorophyll and carotenoids were unaffected by C_{O_2} at sub-saturating and near-saturating light intensities [9]. All of those results confirm that no significant light stress was obtained in all our experiments.

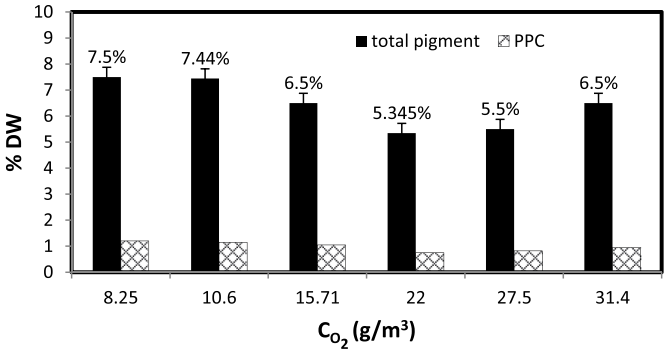

Fig. 3. Evolution of total pigment and photoprotective carotenoid (PPC) contents of *Chlorella vulgaris* at different dissolved oxygen concentrations (C_{O_2}) for a photon flux density PFD = 250 µmol/m²/s (data are shown as mean ± SD n = 3).

3.2. Determination of J_{NADH_2} as a function of C_{O_2}

In Sections 3.1.2 and 3.1.3, it has been shown that photorespiration and photosynthetic activities were not the reason of the biomass productivity loss. Hence, one can suppose that the energy dissipation was due to a change in respiratory activity. Therefore, assuming that C_{O_2} influences respiration rate, it can be related to J_{NADH_2} that represents the respiration activity in the kinetic growth model (Eq. (4)). J_{NADH_2} was then retrieved from the growth model for the different experiments (Eq. (8)).

Fig. 4 presents J_{NADH_2} values from experimentally-measured productivities obtained at the different C_{O_2}. When inhibition did not occur ($C_{O_2} < 30\ g/m^3$), the specific rate of respiratory cofactor regeneration (J_{NADH_2}) was around 2 $mol_{NADH2}/kg_{biomass}/h$ with a progressive increase from 1.8 to 3 $mol_{NADH2}/kg_{biomass}/h$. However, at higher C_{O_2}, the rate increases to reach around 10 $mol_{NADH2}/kg_{biomass}/h$, highlighting a sudden increase of respiration activity at this high C_{O_2}.

3.3. Modeling the influence of C_{O_2} on kinetic growth

3.3.1. Modeling biomass productivity as a function of C_{O_2}

As explained in the Appendix, modeling PBR performances requires coupling photosynthetic growth to the physical phenomenon as light transfer inside the culture volume. The light attenuation field was determined using the two-flux approach [35]. This model requires the determination of the radiative properties of the microalgae strain. Only pigment content, size distribution and shape of cultivated microalgae need to be measured for that purpose. Here we applied the approach described by Kandilian et al. [36]. Radiative properties were calculated by applying Lorenz-Mie theory. Note that the parameters could be validated by transmittance measurement using an integrated sphere photometer and comparing the results with predictive theoretical values [36].

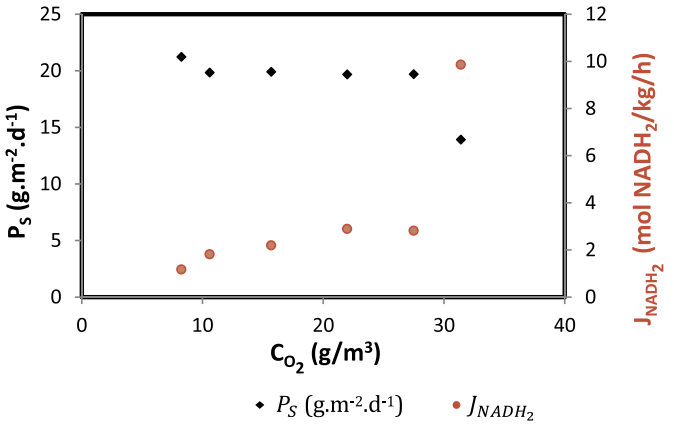

Fig. 4. Evolution of the rate of respiratory cofactor regeneration (J_{NADH_2}) in comparison with the evolution of the surface productivity (P_S) of *Chlorella vulgaris* for different dissolved oxygen concentrations.

In our study, C_{O_2} showed no significant influence on the pigment contents of the microalgae (Fig. 3). This allows us to consider that the database of radiative properties described in Souliès et al. [17], which was obtained from the procedure described by Kandilian et al. [36]. According to this database, a single measurement of pigment concentration was sufficient to retrieve corresponding radiative properties of *Chlorella vulgaris* (see Souliès et al. [17] for these corresponding values).

Since pigment content was only slightly affected, the photosynthetic apparatus of the cells could be supposed undamaged. We thus supposed that parameters of the model related to photosynthetic term (ρ_M, $\overline{\phi'}_{O_2}$, K) were the same as determined by [17]. As a result, only J_{NADH_2} was modified as a function of C_{O_2}. By introducing J_{NADH_2} calculated from the previous section, surface productivity for each C_{O_2} was re-calculated using Eqs. (4) and (5).

Fig. 5(A) shows predicted surface productivities as a function of dilution rate for different C_{O_2} levels (PFD = 200 µmol/m^2/s). Note that in each case, maximal surface productivity was obtained for a different optimal dilution rate value. In a range of non-inhibitory C_{O_2} spanning 8 g/m^3 < C_{O_2} < 27 g/m^3, optimal dilution rate was around 0.035–0.045 h^{-1}. On the other hand, in a range of inhibitory C_{O_2} (i.e. $C_{O_2} \geq 31$ g/m^3), optimal dilution rate was 0.06 h^{-1}. Note too that the model predicts a 25% increase in surface productivity at low C_{O_2} compared to high C_{O_2} (*i. e.*$C_{O_2} \geq 31$ g/m^3).

3.3.2. *Validation of the light-limited kinetic growth model in different* C_{O_2}

Souliès et al. [17] established the kinetic growth model of *Chlorella vulgaris* in the same PBR geometry as used here (i.e. a torus PBR) but without monitoring C_{O_2}, so with an unknown C_{O_2} value. By comparing their results to our model prediction for different C_{O_2} (8 g/m^3 and 31 g/m^3), we were able to estimate the oxygen environment applied in Souliès et al. [17].

The discrepancies between model prediction and experimental values are given in Fig. 5(B), for both high (31 g/m^3) and low (8 g/m^3) C_{O_2}

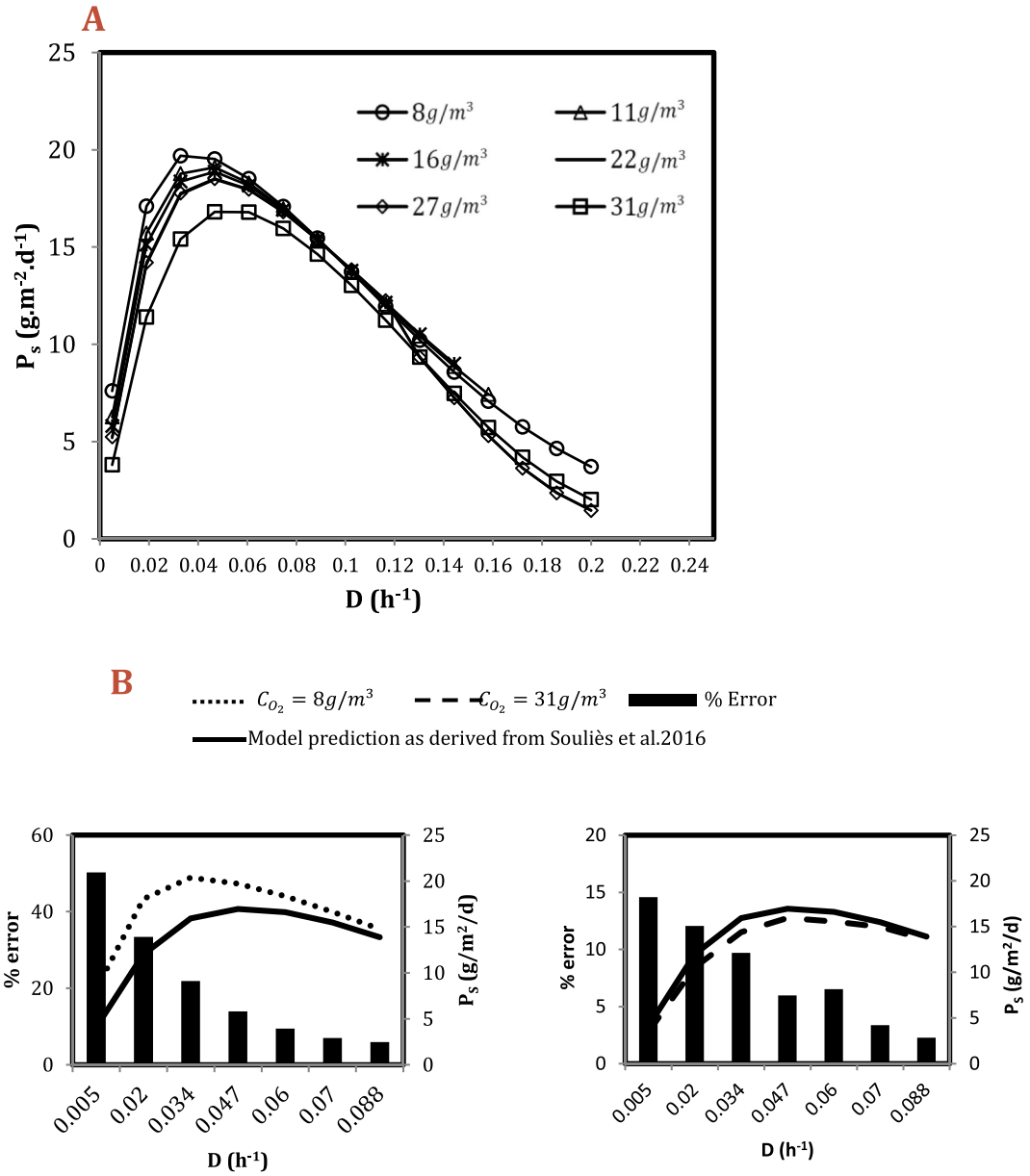

Fig. 5. (A): Prediction of biomass surface productivity of *Chlorella vulgaris* for different dissolved oxygen concentrations using recalculated J_{NADH_2} values. (B): Comparison between experimental surface productivity of *Chlorella vulgaris* obtained by Souliès et al. [17] and theoretical surface productivity recalculated from the kinetic growth model for different dissolved oxygen concentrations and for a photon flux density PFD = 200 µmol/m^2/s.

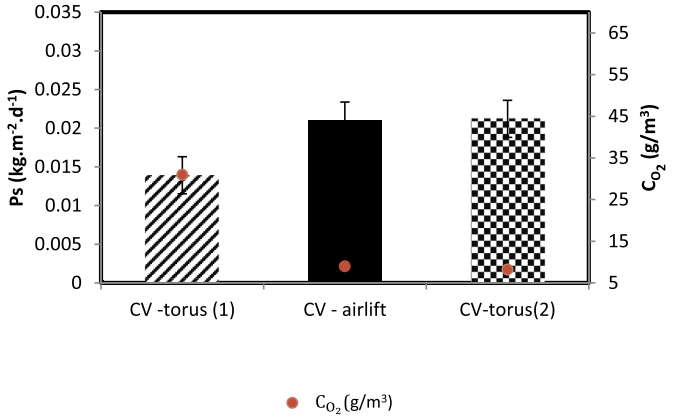

Fig. 6. Surface productivity in airlift and torus PBR for *Chlorella vulgaris* (CV) grown in the two PBRs for a photon flux density PFD = 250 µmol/m^2/s and dilution rate D = 0.02 h^{-1} with different dissolved oxygen concentrations. Values for dissolved oxygen concentrations were added for each case (data are shown as a mean ± SD, n = 3).

values. This tends to show that model parameters from Souliès et al. [17] were obtained in the range of inhibitory C_{O_2} (31 g/m^3). Indeed, errors did not exceed 15% for the different dilution rates in the condition of a C_{O_2} = 31 g·m^{-3}, whereas prediction error was significantly higher at lower C_{O_2} (8 g·m^{-3}). Moreover, in all cases, the error was higher for low dilution rates (50% at low C_{O_2} for a dilution rate D of 0.005 h^{-1}, 30% and 20% for dilution rates of 0.02 and 0.035 h^{-1} respectively, Fig. 5B). This tends to indicate a more marked effect of C_{O_2} for low dilution rate values (between 0.005 h^{-1} and 0.035 h^{-1}). This conclusion has to be related to some of the conclusions of Souliès et al. [17] and Takache et al. [18] who observed that the kinetic growth model was less accurate in such conditions, which they attributed to the formulation of the terms related to respiration activity. Our analysis tends to confirm this explanation, while providing new insight into its direct relation to C_{O_2}. Indeed, the decrease in dilution rate results in an increase in light attenuation conditions because of the higher biomass concentration then obtained. This decreases the contribution of photosynthetic activity in the PBR volume (i.e. less light observed per cells) while increasing the contribution of respiratory activity. As a consequence, an inaccurate representation of the J_{NADH_2} term leads to a higher discrepancy in model prediction for lower dilution rates. The kinetic growth model, as previously formulated (constant J_{NADH_2} value), was then unable to accurately represent the full range of dilution rate values. This hypothesis will be confirmed in the following section.

3.4. Analysis for various lab-scale and industrial photobioreactors

3.4.1. Biomass surface productivity for torus and airlift photobioreactors

Surface productivity has been determined for the microalgae *Chlorella vulgaris* (CV) in two different PBR geometries with the final aim of generalizing our conclusion on the effect of C_{O_2}. Biomass productivity was found 30% higher in the airlift PBR than the torus PBR for the same conditions (PFD = 250 µmol/m^2/s and D = 0.02 h^{-1} (Fig. 6). This discrepancy between the two PBR geometries contradicts one important statement of PBR performances in light-limited conditions, which is that surface productivity is only affected by PFD for a given species (see in Appendix, Eq. (A.6); also see Lee et al. [37]. We then led further analysis on a possible effect of C_{O_2}.

Table 1 presents results of the gas-liquid mass transfer determination for both the torus and airlift PBRs, as obtained by the de-oxygenation/re-oxygenation method. These results were used to estimate the capacity of each PBR to accumulate dissolved oxygen (Eq. (14)). The results, given in Table 1 (see next section for calculation details), show that the two geometries present different gas-liquid transfer efficiencies, and then different C_{O_2} values for a given set of operating conditions. As already explained, the torus PBR allows to modulate gas-liquid mass transfer performances within a wide range, but in our experiments, the typical range of aeration in the torus PBR was around 30 mL/min airflow rate. This is a rather low value with then low gas-liquid mass transfer rate (K_La = 1.13 h^{-1}), when in practice C_{O_2} can accumulate up to values presenting an inhibitory activity (C_{O_2} = 30 g/m^3). In sharp contrast, the typical range of aeration of the airlift PBR was around 400 mL/min airflow rate (K_La = 10 h^{-1}). At this flowrate, C_{O_2} was always found at near-air-saturated values (C_{O_2} = 12 g/m^3, Table 1).

To assess the hypothesis that the airlift PBR presents near-saturating C_{O_2} values whereas the torus PBR presents near-inhibitory C_{O_2} values, cultures of *Chlorella vulgaris* were repeated in the torus PBR but while changing the aeration rate. A value of 200 mL/min was necessary in order to increase gas-liquid mass transfer performance C_{O_2} in near-air-saturated values in the torus PBR, as obtained in the airlift PBR. Results show (Fig. 6) that surface productivity for *Chlorella vulgaris* was found similar in both geometries. This validates our statement that dissolved

Table 1
Gas-liquid mass transfer coefficients and resulting estimated dissolved oxygen concentrations for different photobioreactor geometries (P_{Smax} = 19.5 g/m^2/d).

PBR geometry	P_X (g/m^3/h)	Gas flow/agitation conditions	k_La (h^{-1})	C_{O_2} (g/m^3)	Reference
Torus PBR	0.78	30 mL/min	1.13	35	This study
		50 mL/min	1.7	26	
		100 mL/min	2.76	19	
		500 mL/min	9.03	11	
Flat-panel airlift (1 L)	0.63	50 mL/min	1.9	29	This study
		100 mL/min	3	21	
		400 mL/min	10	12	
		600 mL/min	13.2	11	
Tubular airlift (6 L)	0.96	30 mL/min	5.1	20	[38]
		100 mL/min	10.6	13.9	
		500 mL/min	27.8	10.4	
		1200 mL/min	47.1	9.5	
Raceway	0.19	6 rpm	0.2377	59	[39]
		16 rpm	0.75	24	
		20 rpm	0.97	20	
Tubular horizontal PBR	2.3	–	3.6	48.2	[28]
Near-horizontal PBR	2.88	–	K_La_{min} = 3	68.2	[40]
			K_La_{max} = 7	33.9	
Flat-panel airlift (50 L)	0.14	–	K_La_{min} = 1	16.6	[41]
		–	K_La_{max} = 29	8.5	

oxygen directly influences biomass growth, while confirming that surface productivity is independent of PBR design and is solely light-limited conditions (i.e. no inhibitory effect of C_{O_2}).

3.4.2. Practical guidelines for PBR operation

Experiments in the torus PBR showed that gas flowrate should be maintained at a minimum of around 50 mL/min in order to maintain a healthy environment for the microalgae (C_{O_2} = 30 g/m^3), but should not exceed a maximum of 100 mL/min as there is a risk of CO_2 limitation due to excessive degassing, which results in low C_{O_2} (data not shown). In the case of the 1 L airlift PBR, a minimum gas flowrate of 100 mL/min is recommended to maintain good mixing conditions. In practice, gas flowrate used is generally near 400 mL/min. With this flowrate, accumulation of dissolved oxygen is negligible, so the airlift system remains efficient in terms of oxygen stripping, whatever the aeration rate applied in practice.

Our analysis was extended to other typical microalgal culture systems. Considering that the surface productivity of a microalgal strain remains the same for any PBR design (see Appendix), we calculated volumetric productivity (P_X) depending on the PBR specific illuminated surface following Eq. (A.7). The optimal surface productivity obtained in this study was used as reference value for all cases (19.5 g/m^2/d, Fig. 2). The gas-liquid mass transfer efficiency of different industrial PBRs was collected from the literature in order to estimate C_{O_2} using Eq. (14).

Table 1 summarizes the different C_{O_2} and k_La values obtained for the different PBR geometries. Comparing results, we see that tubular photobioreactors and raceway photobioreactors present a greater capacity to accumulate C_{O_2} than airlift-system photobioreactors. Assuming systems may lose biomass productivity at C_{O_2} > 30 g/m^3 (Fig. 2), culture system technologies such as raceway and tubular PBRs could inhibit biomass growth due to insufficient gas-liquid mass transfer efficiency (our results point to a roughly 30% decrease in biomass productivity). Note that this same interpretation has been confirmed experimentally by many authors [13,15,41–43].

4. Conclusion

Dissolved oxygen concentration C_{O_2} was found to have a negative effect on microalgal growth. A C_{O_2} over 30 g/m^3 was found to induce a 30% loss in biomass productivity on *Chlorella vulgaris*. This was modeled through an increase of the respiratory activity, as given by J_{NADH_2} in our kinetic growth model. The latter increased from about 2 mol/$NADH_2$·kg^{-1}·h^{-1} for 9 < C_{O_2} < 27 g·m^{-3} to 10 mol/$NADH_2$·kg^{-1}·h^{-1} for C_{O_2} = 30 g·m^{-3} where the loss of biomass productivity occurred.

Since oxygen accumulation in culture systems could be avoided by an effective stripping through a better mass transfer efficiency, our analysis was then extrapolate to different culture systems. Considering its efficient gas-liquid mass transfer performance, airlift technology (k_{La} > 10 h^{-1}) was not found to be subjected to dissolved oxygen accumulation. Contrariwise, tubular PBRs and raceways having k_{La} < 7 h^{-1} presented dissolved oxygen accumulation, which could reach concentration leading to a negative impact on biomass productivity. The presence of degassers is then crucial for controlling this parameter in those technologies.

Abbreviations

PBR	Photobioreactor
PFD	Photon flux density; total radiation received on the photobioreactor surface [µmol·m^{-2}·s^{-1}]
D	Dilution rate [h^{-1}]
L_Z	Depth of culture [m]
V_{PBR}	Volume of the PBR [m^3]
S_V	Illuminated area of the photobioreactor [m^2]
a_{light}	Specific illuminated area for the photobioreactor [m^{-1}]
J_{O_2}	Local specific rate of oxygen production or consumption [mol$_{O2}$kg$_X^{-1}$ s^{-1}]
$J_{O_2,\ photo}$	Local rate of oxygen production due to photosynthesis [mol$_{O2}$kg$_X^{-1}$ s^{-1}]
$J_{O_2,\ resp}$	Local rate of oxygen consumption due to respiration [mol$_{O2}$kg$_X^{-1}$ s^{-1}]
ρ_M	Maximum energy yield for photon conversion [dimensionless]
$\overline{\phi'}_{O_2}$	Mean mass quantum yield for the *Z*-scheme of photosynthesis [mol$_{O2}$·µmol$_{h\nu}^{-1}$]
K	Half saturation constant for photosynthesis [µmol$_{h\nu}$kg^{-1} s^{-1}]
A	Local specific rate of photon absorption [µmol$_{h\nu}$kg^{-1} s^{-1}]
J_{NADH_2}	Rate of cofactor regeneration in the respiratory chain of the microalgae [mol$_{NADH2}$·kg^{-1}·h^{-1}]
$\nu_{NADH_2-O_2}$	Stoichiometric coefficient of cofactor regeneration on the respiratory chain [dimensionless]
K_r	Half saturation constant describing the inhibition by respiration [µmol·kg^1·s^{-1}]
r_X	Rate of biomass production [kg·m^{-3}·d^{-1}]
ν_{O_2-X}	Stoichiometric coefficient of the oxygen production [dimensionless]
C_X	Biomass concentration [kg·m^{-3}]
M_X	C-molar mass for the biomass [kg$_X$·mol$_X^{-1}$]
P_X	Volumetric biomass productivity [kg·m^{-3}·d^{-1}]
P_S	Surface biomass productivity [kg·m^{-2}·d^{-1}]
r	Ratio of photorespiration [no unit]
DIC	Dissolved inorganic carbon [mol·L^{-1}]
K'	Dissociation constant of CO_2 in water [no unit]
N_{O_2}	Oxygen mass transfer rate [kg·m^{-3}·s^{-1}]
K_La	Gas-liquid mass transfer coefficient [h^{-1}]
C_{O_2}	Dissolved oxygen concentration [g·m^{-3}]
$C_{O_2}^*$	Dissolved oxygen concentration at equilibrium with the gas phase [8.25 g·m^{-3} at 25 °C]
$Y_{O_2/X}$	Specific yield of oxygen production [dimensionless]
P_{O_2}	Oxygen volumetric productivity [kg·m^{-3}·s^{-1} or kg·m^{-3}·h^{-1}]

Declaration of authors' contributions

The manuscript has been read and approved by all named authors and that there are no other persons who satisfied the criteria for authorship but are not listed. We further confirm that the order of authors listed in the manuscript has been approved by all of us.

Antoinette Kazbar was the main contributor of this work. Her contribution was on the conception and design of the study, or acquisition of data, or analysis and interpretation of data; drafting the article or revising it critically for important intellectual content; final approval of the version to be submitted.

Jeremy Pruvost was involved in the conception and design of the study, or acquisition of data, or analysis and interpretation of data; drafting the article or revising it critically for important intellectual content; final approval of the version to be submitted.

Guillaume Cogne contributed on the analysis and interpretation of the data, drafting of the article, critical revision of the article for important intellectual content and final approval of the article.

Benjamin Le Gouic, Jordan Tallec and Brieuc Urbain contributed on the collection and assembly of data.

Hélène Marec contributed on the conception and design of the experimental setups.

Hosni Takache and Ali Ismail contributed on the final approval of the article and administrative, technical, or logistic support.

Conflict of interest statement

There are no known conflicts of interest associated with this publication and there has been no significant financial support for this work that could have influenced its outcome.

Statement of informed consent, human/animal rights

No conflicts, informed consent, human or animal rights applicable.

Acknowledgments

This research did not receive any specific grants from funding agencies in the public, commercial, or not-for-profit sectors.

Appendix A

A.1. Description of the kinetic growth model

Pruvost et al. [16] proposed a model that relates light attenuation conditions to photosynthetic growth. This model was consolidated in Souliès et al. [17]. It allows to predict photobioreactor performance or productivity variation for operating parameters affecting light-limited cultures (residence time, PFD, etc.). It is based on the determination of the local oxygen production rate (J_{O_2}) that requires the RPA (rate of photon absorption) field to be known. This RPA (A) field is a function of PBR geometry, light source, cell optical properties, and biomass concentration. In our case, light attenuation in the culture volume occurs mainly in one direction. It can then be modeled using the two-flux radiative model [16,35]. This makes it possible to predict the irradiance field by:

$$\frac{G_\lambda(z)}{q_{\lambda,0}} = 2\frac{[\rho(1+\alpha_\lambda)e^{-\delta_\lambda L} - (1-\alpha_\lambda)e^{-\delta_\lambda L}]e^{\delta_\lambda L} + [(1+\alpha_\lambda)e^{\delta_\lambda L} - \rho(1-\alpha_\lambda)e^{\delta_\lambda L}]e^{-\delta_\lambda L}}{(1+\alpha_\lambda)^2 e^{\delta_\lambda L} - (1-\alpha_\lambda)^2 e^{-\delta_\lambda L} - \rho(1-\alpha_\lambda{}^2)e^{\delta_\lambda L} + \rho(1-\alpha_\lambda{}^2)e^{-\delta_\lambda L}} \tag{A.1}$$

In this equation, $\alpha_\lambda = \sqrt{\frac{Ea_\lambda}{Ea_\lambda + 2b_\lambda \cdot Es_\lambda}}$ is the linear scattering modulus, and $\delta_\lambda = C_X\sqrt{Ea_\lambda\,(Ea_\lambda + 2b_\lambda \cdot Es_\lambda)}$ is the two-flux extension coefficient. These values are obtained from the radiative properties of the cultivated cells, namely $E_{a\lambda}$, $E_{s\lambda}$ and b_λ, which are the mass absorption coefficient, mass scattering coefficient and backscattered fraction, respectively, expressed here for a given wavelength. Setpoint radiative properties could be predicted theoretically using pigment content and cell shape and size distribution [35] or by experimental measurements [36]. For *Chlorella vulgaris*, a complete database is available in Souliès et al. [17].

The determination of the irradiance field can be used to calculate light absorbed by biomass, as represented by the specific rate of photon absorption, A (RPA), which represents the light effectively absorbed by the cells and is thus the combination of the light received, represented by the irradiance G ($\mu mol_{hv}/m^2/s$), and the ability of the cells to absorb light, as represented by the mass absorption coefficient E_a (m^2/kg). The specific RPA is then given by:

$$A = E_a \cdot G \tag{A.2}$$

Determining the local RPA makes it possible to predict the corresponding photosynthetic growth rate, expressed here as a rate of oxygen production J_{O_2}:

$$J_{O_2} = \rho_M \frac{K}{K+A}\bar{\phi}'_{O_2} A - \frac{J_{NADH_2}}{\nu_{NADH_2-O_2}} \cdot \frac{Kr}{Kr+A} \tag{A3}$$

where ρ is energy yield for photon conversion of maximum value ρ_M, $\overline{\phi}'_{O_2}$ ($molO_2/\mu mol_{hv}$) is molar quantum yield for the *Z*-scheme of photosynthesis as deduced from the structured stoichiometric equations, K ($\mu mol_{hv} \cdot kg^{-1} \cdot s^{-1}$) is half saturation constant for photosynthesis, J_{NADH_2}($mol_{NADH2} \cdot kg^{-1} \cdot s^{-1}$) is specific rate of cofactor regeneration on the respiratory chain in the light, linked here to oxygen consumption by the stoichiometric coefficient $\nu_{NADH_2-O_2}$ (stoichiometric coefficient of cofactor regeneration on the respiratory chain), and K_r ($\mu mol_{hv} \cdot kg^{-1} \cdot s^{-1}$) is half saturation constant describing the inhibition of respiration in light.

As a direct result of the light distribution inside the culture volume, the kinetic relation is of local type. This implies calculating the corresponding mean value ($\langle J_{O_2} \rangle$) by averaging over the total culture volume V_R:

$$\langle J_{O_2} \rangle = \frac{1}{V_R} \iiint_{V_R} J_{O_2}\, dV_R \tag{A.4}$$

Consequently, the mean volumetric biomass growth rate $\langle r_X \rangle$ can be deduced by:

$$\langle r_X \rangle = \frac{< J_{O_2} > C_X M_X}{\nu_{O_{2-x}}} \tag{A.5}$$

where M_X is C-molar mass of the biomass (kg/mol) and $\nu_{O_{2-x}}$ is stoichiometric coefficient of oxygen production.

Finally, once the mean volumetric growth rate is known, the resolution of the mass balance equation for biomass (Eq. (7)) can serve to calculate biomass concentration and productivity as a function of operating parameters (PFD, D).

A.2. Predicting photobioreactor kinetic performances

Cornet & Dussap [44] developed a predictive engineering formula for the assessment of kinetic and energetic performances of a photobioreactors as a function of their design. This formula gives the maximum volumetric and surface biomass productivities by assuming (i) that light is the only limiting factor and (ii) that the culture system is operated at an optimal biomass concentration leading to optimal light attenuation conditions. This leads to the simplified engineering formulas giving maximal surface (P_{Smax}) and volumetric biomass productivity (P_{Xmax}), respectively:

$$P_{S_{max}} = (1-f_d)\overline{\phi}'_X \cdot \rho_M \cdot M_X \frac{2\alpha}{1+\alpha} K\, ln\left[1 + \frac{q_0}{K}\right] \tag{A.6}$$

where P_{Smax} is maximum surface productivity, f_d is dark fraction (representing an unilluminated volume of the photobioreactor due to its design), $\overline{\phi}'_X$ is mean mass quantum yield of the *Z*-scheme of photosynthesis ($\overline{\phi}'_X = \frac{M_X \cdot \overline{\varphi}'_{O_2}}{\nu_{O_2-X}}$), ρ_M is energy yield for photon conversion of maximum value, K is half saturation constant for photosynthesis, M_x is molar mass of the strain used in the study, q_0 is total collected flux density (PFD)and α is linear scattering modulus relating to the microorganism's radiative properties. Note that this equation indicates that surface productivity is only affected by

PFD for a given species. As a result, volumetric productivity can be obtained from surface value, if the specific illuminated surface is known:

$$P_{X_{max}} = P_{S_{max}} \times \frac{S_{light}}{V_R} = P_{S_{max}} \times a_{light} \tag{A.7}$$

where a_{light} is specific illuminated surface as given by the surface-to-volume ratio (m^{-1}).

Here we used these equations to estimate the maximal performances of various PBR geometries in the final part of this work. By setting a given value of surface productivity, we were able to deduce volumetric productivity assuming the same light received (q_0) and using the characteristics of the cultivated strains. Note also that Eqs. (A.6) and (A.7) correspond to specific culture conditions, i.e. light-limited growth with full light attenuation and no dark volumes ([16,18,46,47]. They do not consider the possible effect of dissolved oxygen concentration.

References

[1] A.M.J. Kliphuis, D.E. Martens, M. Janssen, R.H. Wijffels, Effect of O_2:CO_2 ratio on the primary metabolism of *Chlamydomonas reinhardtii*, Biotechnol. Bioeng. 108 (2011) 2390–2402, https://doi.org/10.1002/bit.23194.

[2] J.V. Moroney, N. Jungnick, R.J. DiMario, D.J. Longstreth, Photorespiration and carbon concentrating mechanisms: two adaptations to high O_2, low CO_2 conditions, Photosynth. Res. 117 (2013) 121–131, https://doi.org/10.1007/s11120-013-9865-7.

[3] H. Bauwe, M. Hagemann, R. Kern, S. Timm, Photorespiration has a dual origin and manifold links to central metabolism, Curr. Opin. Plant Biol. 15 (2012) 269–275, https://doi.org/10.1016/j.pbi.2012.01.008.

[4] V.G. Maurino, C. Peterhansel, Photorespiration: current status and approaches for metabolic engineering, Curr. Opin. Plant Biol. 13 (2010) 248–255, https://doi.org/10.1016/j.pbi.2010.01.006.

[5] G. Torzillo, A. Vonshak, Environmental stress physiology with reference to mass cultures, in: Amos Richmond, Qiang Hu (Eds.), Handbook of Microalgal Culture, John Wiley & Sons, Ltd, 2013, pp. 90–113.

[6] M.R. Badger, S. von Caemmerer, S. Ruuska, H. Nakano, Electron flow to oxygen in higher plants and algae: rates and control of direct photoreduction (Mehler reaction) and rubisco oxygenase, Philos. Trans. R. Soc. B 355 (2000) 1433–1446.

[7] A.H. Mehler, Studies on reactions of illuminated chloroplasts, Arch. Biochem. Biophys. 33 (1951) 65–77, https://doi.org/10.1016/0003-9861(51)90082-3.

[8] S. Raso, B. van Genugten, M. Vermuë, R.H. Wijffels, Effect of oxygen concentration on the growth of Nannochloropsis sp. at low light intensity, J. Appl. Phycol. 24 (2012) 863–871, https://doi.org/10.1007/s10811-011-9706-z.

[9] C. Sousa, A. Compadre, M.H. Vermuë, R.H. Wijffels, Effect of oxygen at low and high light intensities on the growth of *Neochloris oleoabundans*, Algal Res. 2 (2013) 122–126, https://doi.org/10.1016/j.algal.2013.01.007.

[10] T.A. Costache, F.G.A. Fernández, M.M. Morales, J.M. Fernández-Sevilla, I. Stamatin, E. Molina, Comprehensive model of microalgae photosynthesis rate as a function of culture conditions in photobioreactors, Appl. Microbiol. Biotechnol. 97 (2013) 7627–7637, https://doi.org/10.1007/s00253-013-5035-2.

[11] T. Genkov, R.J. Spreitzer, Highly conserved small subunit residues influence rubisco large subunit catalysis, J. Biol. Chem. 284 (2009) 30105–30112, https://doi.org/10.1074/jbc.M109.044081.

[12] E. Molina Grima, F.G.A. Fernández, F. Garcia Camacho, Y. Chisti, Photobioreactors: light regime, mass transfer, and scaleup, J. Biotechnol. 70 (1999) 231–247, https://doi.org/10.1016/S0168-1656(99)00078-4.

[13] C. Posten, Design principles of photo-bioreactors for cultivation of microalgae, Eng. Life Sci. 9 (2009) 165–177, https://doi.org/10.1002/elsc.200900003.

[14] F.J. Marquez, K. Sasaki, N. Nishio, S. Nagai, Inhibitory effect of oxygen accumulation on the growth of Spirulina platensis, Biotechnol. Lett. 17 (1995) 225–228, https://doi.org/10.1007/BF00127993.

[15] J.C. Weissman, R.P. Goebel, J.R. Benemann, Photobioreactor design: mixing, carbon utilization, and oxygen accumulation, Biotechnol. Bioeng. 31 (1988) 336–344, https://doi.org/10.1002/bit.260310409.

[16] J. Pruvost, J.F. Cornet, V. Goetz, J. Legrand, Theoretical investigation of biomass productivities achievable in solar rectangular photobioreactors for the cyanobacterium Arthrospira platensis, Biotechnol. Prog. 28 (2012) 699–714, https://doi.org/10.1002/btpr.1540.

[17] A. Souliès, J. Legrand, H. Marec, J. Pruvost, C. Castelain, T. Burghelea, J.-F. Cornet, Investigation and modeling of the effects of light spectrum and incident angle on the growth of *Chlorella vulgaris* in photobioreactors, Biotechnol. Prog. 32 (2016) 247–261, https://doi.org/10.1002/btpr.2244.

[18] H. Takache, J. Pruvost, J.-F. Cornet, Kinetic modeling of the photosynthetic growth of Chlamydomonas reinhardtii in a photobioreactor, Biotechnol. Prog. 28 (2012) 681–692, https://doi.org/10.1002/btpr.1545.

[19] S. Fouchard, J. Pruvost, B. Degrenne, J. Legrand, Investigation of H2 production using the green microalga Chlamydomonas reinhardtii in a fully controlled photobioreactor fitted with on-line gas analysis, Int. J. Hydrog. Energy 33 (2008) 3302–3310, https://doi.org/10.1016/j.ijhydene.2008.03.067.

[20] N. Sueoka, Mitotic replication of deoxyribonucleic acid in *Chmamydomonas reinhardtii*, Proc. Natl. Acad. Sci. U. S. A. 46 (1960) 83–91.

[21] J. Pruvost, J. Legrand, P. Legentilhomme, J.M. Rosant, Numerical investigation of bend and torus flows. Part II: flow simulation in torus reactor, Chem. Eng. Sci. 59 (2004) 3359–3370.

[22] H. Takache, J. Pruvost, H. Marec, Investigation of light/dark cycles effects on the photosynthetic growth of Chlamydomonas reinhardtii in conditions representative of photobioreactor cultivation, Algal Res. 8 (2015) 192–204, https://doi.org/10.1016/j.algal.2015.02.009.

[23] J. Pruvost, G. Van Vooren, B. Le Gouic, A. Couzinet-Mossion, J. Legrand, Systematic investigation of biomass and lipid productivity by microalgae in photobioreactors for biodiesel application, Bioresour. Technol. 102 (2011) 150–158, https://doi.org/10.1016/j.biortech.2010.06.153.

[24] R.J. Ritchie, Consistent sets of spectrophotometric chlorophyll equations for acetone, methanol and ethanol solvents, Photosynth. Res. 89 (2006) 27–41, https://doi.org/10.1007/s11120-006-9065-9.

[25] T.M. Mata, A.A. Martins, N.S. Caetano, Microalgae for biodiesel production and other applications: a review, Renew. Sust. Energ. Rev. 14 (2010) 217–232, https://doi.org/10.1016/j.rser.2009.07.020.

[26] H. Bauwe, M. Hagemann, A.R. Fernie, Photorespiration: players, partners and origin, Trends Plant Sci. 15 (2010) 330–336, https://doi.org/10.1016/j.tplants.2010.03.006.

[27] B. Urbain, Elaboration d'un modèle biochimiquement structuré de la croissance d'une microalgue eucaryote en PBRs: *Chlamydomonas reinhardtii*, University of Nantes, Thesis, 2017.

[28] F.C. Rubio, F.G.A. Fernández, J.A.S. Pérez, F.G. Camacho, E.M. Grima, Prediction of dissolved oxygen and carbon dioxide concentration profiles in tubular photobioreactors for microalgal culture, Biotechnol. Bioeng. 62 (1999) 71–86, https://doi.org/10.1002/(SICI)1097-0290(19990105)62:1<71::AID-BIT9>3.0.CO;2-T.

[29] M. Roustan, Transferts gaz-liquide dans les procédés de traitement des eaux et des effluents gazeux [WWW Document], Libr. Lavoisier, 2003 URL https://www.lavoisier.fr/livre/environnement/transferts-gaz-liquide-dans-les-procedes-de-traitement-des-eaux-et-des-effluents-gazeux/roustan/descriptif-9782743006051 , Accessed date: 15 August 2017.

[30] J. Pruvost, F. Le Borgne, A. Artu, J. Legrand, Development of a thin-film solar photobioreactor with high biomass volumetric productivity (AlgoFilm©) based on process intensification principles, Algal Res. 21 (2017) 120–137, https://doi.org/10.1016/j.algal.2016.10.012.

[31] K. Loubière, E. Olivo, G. Bougaran, J. Pruvost, R. Robert, J. Legrand, A new photobioreactor for continuous microalgal production in hatcheries based on external-loop airlift and swirling flow, Biotechnol. Bioeng. 102 (2009) 132–147, https://doi.org/10.1002/bit.22035.

[32] C.U. Ugwu, H. Aoyagi, H. Uchiyama, Influence of irradiance, dissolved oxygen concentration, and temperature on the growth of Chlorella sorokiniana, Photosynthetica 45 (2007) 309–311, https://doi.org/10.1007/s11099-007-0052-y.

[33] A. Martzoff, Analyse systémique du métabolisme carboné et énergétique de *Chlamydomonas reinhardtii* (Thesis), University of Nantes, 2013.

[34] A. Richmond, Amos Richmond, Qiang Hu (Eds.), Wiley: Handbook of Microalgal Culture: Applied Phycology and Biotechnology, 2nd edition, 2004 [www document]. URL http://www.wiley.com/WileyCDA/WileyTitle/productCd-0470673893.html , Accessed date: 14 August 2017.

[35] L. Pottier, J. Pruvost, J. Deremetz, J.-F. Cornet, J. Legrand, C.G. Dussap, A fully predictive model for one-dimensional light attenuation by Chlamydomonas reinhardtii in a torus photobioreactor, Biotechnol. Bioeng. 91 (2005) 569–582, https://doi.org/10.1002/bit.20475.

[36] R. Kandilian, J. Pruvost, A. Artu, C. Lemasson, J. Legrand, L. Pilon, Comparison of experimentally and theoretically determined radiation characteristics of photosynthetic microorganisms, J. Quant. Spectrosc. Radiat. Transf. 175 (2016) 30–45, https://doi.org/10.1016/j.jqsrt.2016.01.031.

[37] E. Lee, J. Pruvost, X. He, R. Munipalli, L. Pilon, Design tool and guidelines for outdoor photobioreactors, Chem. Eng. Sci. 106 (2014) 18–29, https://doi.org/10.1016/j.ces.2013.11.014.

[38] K. Loubière, J. Pruvost, F. Aloui, J. Legrand, Investigations in an external-loop airlift photobioreactor with annular light chambers and swirling flow, Chem. Eng. Res. Des. 89 (2011) 164–171, https://doi.org/10.1016/j.cherd.2010.06.001.

[39] B. Le Gouic, Analyse et optimisation de l'apport de carbone en photobioréacteur (Thesis), University of Nantes, 2013.

[40] R.W. Babcock, J. Malda, J.C. Radway, Hydrodynamics and mass transfer in a tubular airlift photobioreactor, J. Appl. Phycol. 14 (2002) 169–184, https://doi.org/10.1023/A:1019924226457.

[41] R. Reyna-Velarde, E. Cristiani-Urbina, D.J. Hernández-Melchor, F. Thalasso, R.O. Cañizares-Villanueva, Hydrodynamic and mass transfer characterization of a flat-panel airlift photobioreactor with high light path, Chem. Eng. Process. Intensif. 49 (2010) 97–103, https://doi.org/10.1016/j.cep.2009.11.014.

[42] M.A. Borowitzka, N.R. Moheimani, Sustainable biofuels from algae, Mitig. Adapt. Strateg. Glob. Chang. 18 (2013) 13–25, https://doi.org/10.1007/s11027-010-9271-9.

[43] D.O. Hall, F.G. Acién Fernández, E.C. Guerrero, K.K. Rao, E.M. Grima, Outdoor helical tubular photobioreactors for microalgal production: modeling of fluid-

dynamics and mass transfer and assessment of biomass productivity, Biotechnol. Bioeng. 82 (2003) 62–73, https://doi.org/10.1002/bit.10543.
[44] J.-F. Cornet, C.-G. Dussap, A simple and reliable formula for assessment of maximum volumetric productivities in photobioreactors, Biotechnol. Prog. 25 (2009) 424–435, https://doi.org/10.1002/btpr.138.
[45] Y. Chisti, Large-scale production of algal biomass: raceway ponds, Algae Biotechnology, Green Energy and Technology. Springer, Cham, 2016, pp. 21–40, , https://doi.org/10.1007/978-3-319-12334-9_2.
[46] J. Pruvost, J.F. Cornet, F. Le Borgne, V. Goetz, J. Legrand, Theoretical investigation of microalgae culture in the light changing conditions of solar photobioreactor production and comparison with cyanobacteria, Algal Res. 10 (juillet) (2015) 87–99, https://doi.org/10.1016/j.algal.2015.04.005.
[47] J. Pruvost, F. Le Borgne, A. Artu, J.-F. Cornet, J. Legrand, Chapter Five - Industrial Photobioreactors and Scale-Up Concepts. In Advances in Chemical Engineering, in: J. Legrand (Ed.), Photobioreaction Engineering, 48 Academic Press, 2016, pp. 257–310.